CHAPTER-9

SELF-FOCUSING OF HERMITE-COSINE- GAUSSIAN LASER BEAM IN PLASMA UNDER DENSITY TRANSITION

9.1 INTRODUCTION

The self-focusing of laser beams in a nonlinear medium like plasma is a captivating field of research which has an excellence in both theoretical and experimental fields [8, 12]. The intensity of the laser beam, sensitivity of decentered of decentered parameter b and density transition are considered to have a crucial role and having interesting qualities in self-focusing [22, 90]. During the propagation of a laser beam in a Kerr medium, the central parts of the beam give rise to radial compression and the cos-Gaussian beam eventually converts in to a cosh-Gaussian type beam with moderate power [27]. In weakly relativistic and ponderomotive regime, a large value of absorption level weakens the self-focusing effect in the absence of decentered parameter. However, oscillatory self-focusing occurs for a higher value of decentered parameter and all curves are seen to demonstrate self-focusing in a sharp manner [21]. In ponderomotive self-focusing, it is the density ramp that results in sooner and better self-focusing [77]. Furthermore, the quantum effect plays a crucial role in making it earlier and stronger as compared to classical one [84]. Again, apart from quantum effects, the upward ramped density profile results in higher oscillations of beam width parameter and consequently in sooner and better focusing [82]. Nanda *et al.* [91] found that the optimized laser and plasma parameters are equally important to obtain better focusing [93]. Patil *et al*. [135] predicted that the thermal quantum effects are equally important for more oscillations of beam-width parameter. However, it was found that in presence of the multiply charged ions, the nonlinear effects get reduced and hence self-focusing becomes less pronounced [136]. Gupta *et al.* [87] found that it is important to consider the ion temperature for the thermal self-focusing. Furthermore, the upward density transition can accelerate the electron to higher energy over a long propagation distance in comparison to uniform density relativistic plasma [85]. Again, Kant and Wani [118] found that the phenomenon of self-focusing is enhanced by decentered parameter and density transition. Moreover, the oscillatory self-

focusing takes place for decentered parameter b ≤ 2 [106]. It is to be noted that the optimization of intensity parameter and wavelength can help in obtaining sooner and strong self-focusing [94].

We previously studied the self-focusing of Hermite-cosh-Gaussian beam in plasma and observed that these beams give freedom to mode index (m) and decentered parameter (b). But, it was possible only up to the decentered parameter $b \leq 1$ [119]. Thereafter, Wani and Kant [130] investigated the relativistic self-focusing of HcosG beam in collisionless plasma. They reported that the beam width parameter shows a strong oscillatory behavior and hence the laser beam becomes more focused at lower values of decentered and intensity parameters. However, in the present communication, our purpose is to analyze the impact of upward plasma density ramp profile $n(\xi) = n_0 \tan(\xi / d)$ on self-focusing of HcosG beam propagating in underdense plasma which was not done earlier for such a beam. The importance of the present work lies in the fact that the density transition causes more reduction in the amplitude of spot size of laser beam close to the propagation axis. Therefore, the minimum spot size of the beam decreases and hence modulates the phenomenon of self-focusing. Above all in the present analysis the decentered parameter has a noticeable impact on the propagation of HcosG beam. The present analysis employs WKB and paraxial approximations and is based on the parabolic wave equation approach [114]. The non-linear dielectric constant of plasma is presented in ponderomotive regime. The equations that govern the laser spot size are derived. The computational results in context of plasma density ramp and decentered parameter are discussed and finally a brief conclusion is added.

9.2 FIELD DISTRIBUTION OF HERMITE – COSINE – GAUSSIAN (HcosG) BEAM

Considering the Hermite-cosine-Gaussian (HcosG) laser beam that propagates in the z direction has the field distribution of the form

$$E(x,y,z) = \frac{E_0}{\sqrt{f_1(z) f_2(z)}} H_m\left(\frac{\sqrt{2}x}{r_0 f_1(z)}\right) H_n\left(\frac{\sqrt{2}y}{r_0 f_2(z)}\right) \exp\left[-\left(\frac{x^2}{r_0^2 f_1^2(z)} + \frac{y^2}{r_0^2 f_2^2(z)}\right)\right] \times \cos\left(\frac{\Omega_0 x}{f_1(z)}\right) \cos\left(\frac{\Omega_0 y}{f_2(z)}\right), \quad (9.1)$$

where, H_m and H_n are the m^{th} and n^{th} order Hermite polynomial respectively, E_0 is the constant

amplitude of the electric field, r_0 is the waist width, Ω_0 is the parameter associated with the cosine function, $f_1(z)$ and $f_2(z)$ are the beam width parameters in respective x and y directions.

9.3 NONLINEAR DIELECTRIC CONSTANT

Consider the propagation of HcosG laser beam in plasma whose dielectric constant is characterized of the form [20]

$$\varepsilon = \varepsilon_0 + \phi(EE^*) \tag{9.2}$$

where, $\varepsilon_0 = 1 - \omega_p^2/\omega^2$ represents the linear part of dielectric constant, $\omega_p^2 = 4\pi n(\xi)e^2/m$, $n(\xi) = n_0 \tan(\xi/d)$ and $\omega_{p0} = \left(4\pi n_0 e^2/m\right)^{1/2}$ is the plasma frequency, e, m and n_0 being the magnitude of the electronic charge, rest mass and electron density respectively, ξ is the normalized propagation distance and d is a dimensionless adjustable parameter. The other part $\phi(EE^*) = (\omega_{p0}^2/\omega^2)\left(1 - \exp(-3m\alpha EE^*/4M)\right)\tan(\xi/d)$ represents the nonlinear part of dielectric constant [28], where, $\alpha = e^2M/6m_0^2\omega^2 k_B T_0$ and M is the scaterrer mass in the plasma, ω is the frequency of laser used, k_B is the Boltzmann constant and T_0 is the equilibrium temperature.

9.4 SELF-FOCUSING EQUATIONS

The wave equation that governs the propagation of laser beam can be of the following form

$$\nabla^2\vec{E} - \frac{\varepsilon}{c^2}\left(-\omega^2\vec{E}\right) + \vec{\nabla}\left(\frac{\vec{E}\vec{\nabla}\cdot\varepsilon}{\varepsilon}\right) = 0 \tag{9.3}$$

The last term of equation (9.3) on left hand side is neglected as $k^{-2}\nabla^2\left(\ln\varepsilon\right) << 1$, where 'k 'represents the wave number the laser beam. Thus,

$$\nabla^2\vec{E} + \frac{\omega^2}{c^2}\varepsilon\vec{E} = 0 \tag{9.4}$$

In Cartesian co-ordinate system, we can write this equation as

$$\frac{\partial^2\vec{E}}{\partial x^2} + \frac{\partial^2\vec{E}}{\partial y^2} + \frac{\partial^2\vec{E}}{\partial z^2} + \varepsilon\frac{\omega^2}{c^2}\vec{E} = 0 \tag{9.5}$$

The solution of equation (9.5) is of the following form,

$$\vec{E} = A(x, y, z)Exp[i(\omega t - kz)] \tag{9.6}$$

With $k^2 = \varepsilon_0 \frac{\omega^2}{c^2} = \frac{\omega^2}{c^2}\left(1 - \frac{\omega_{p0}^2}{\omega^2}\tan(\xi / d)\right)$, (9.6a)

where, $\xi = z/R_d$. Now, differentiating equation (9.6) twice w. r. t.' x, y and z respectively , we get

$$\frac{\partial \vec{E}}{\partial x} = Exp[i(\omega t - kz)]\frac{\partial A}{\partial x}$$

$$\frac{\partial^2 \vec{E}}{\partial x^2} = Exp[i(\omega t - kz)]\frac{\partial^2 A}{\partial x^2}$$

$$\frac{\partial \vec{E}}{\partial y} = Exp[i(\omega t - kz)]\frac{\partial A}{\partial y}$$

$$\frac{\partial^2 \vec{E}}{\partial y^2} = Exp[i(\omega t - kz)]\frac{\partial^2 A}{\partial y^2}$$

Similarly,

$$\frac{\partial^2 \vec{E}}{\partial z^2} = Exp[i(\omega t - kz)]\left[\frac{\partial^2 A}{\partial z^2} + \frac{iA\omega_{p0}^2 Sec^2(z/dR_d)}{2cdR_d\sqrt{\omega^2 - \omega_{p0}^2\tan(z/dR_d)}} + \frac{iA\omega_{p0}^4 zSec^2(z/dR_d)}{4cd^2R_d^2(\omega^2 - \omega_{p0}^2\tan(z/dR_d))^{3/2}}\right]$$

$$+\frac{Exp[i(\omega t - kz)]}{\sqrt{\omega^2 - \omega_{p0}^2\tan(z/dR_d)}}\left[\begin{array}{l}\frac{iA\omega_{p0}^2 zSec^2(z/dR_d)\tan(z/dR_d)}{cd^2R_d^2} + \frac{iA\omega_{p0}^2 zSec^2(z/dR_d)}{2cdR_d} \\ -\frac{i(\omega^2 - \omega_{p0}^2\tan(z/dR_d))}{c}\left(\frac{\partial A}{\partial z}\right) - \frac{i\omega_{p0}^2 zSec^2(z/dR_d)}{2cdR_d}\left(\frac{\partial A}{\partial z}\right)\end{array}\right]$$

$$+\frac{AExp[i(\omega t - kz)]}{c^2}\left[\begin{array}{l}\frac{\omega_{p0}^2 zSec^2(z/dR_d)}{dR_d} - \frac{\omega_{p0}^4 z^2 Sec^4(z/dR_d)}{4d^2R_d^2(\omega^2 - \omega_{p0}^2\tan(z/dR_d))} \\ -(\omega^2 - \omega_{p0}^2\tan(z/dR_d))\end{array}\right]$$

Now, employing the WKB approximation and substituting the above values in Eq. (9.5) and neglecting $(\partial^2 A/\partial z^2)$, we get

$$\frac{\partial^2 A}{\partial x^2}+\frac{\partial^2 A}{\partial y^2}+\frac{\omega^2}{c^2}\Phi(AA^*)A=\frac{i}{c}\left(\frac{2dR_d(\omega^2-\omega_{p0}^2\tan(z/dR_d))-\omega_{p0}^2 z\sec^2(z/dR_d)}{2dR_d\sqrt{\omega^2-\omega_{p0}^2\tan(z/dR_d)}}\right)\left(\frac{\partial A}{\partial z}\right)$$

$$-\frac{iA\omega_{p0}^2\sec^2(z/dR_d)}{cdR_d\sqrt{\omega^2-\omega_{p0}^2\tan(z/dR_d)}}\left(1+\frac{\omega_{p0}^2 z}{4dR_d(\omega^2-\omega_{p0}^2\tan(z/dR_d))}+\frac{z\tan(z/dR_d)}{dR_d}\right)$$

$$-\frac{iA\omega_{p0}^2\sec^2(z/dR_d)}{cdR_d\sqrt{\omega^2-\omega_{p0}^2\tan(z/dR_d)}}\left(\frac{\omega_{p0}^2 z\tan^2(z/dR_d)}{4dR_d(\omega^2-\omega_{p0}^2\tan(z/dR_d))}\right)-\frac{A\omega_{p0}^2 z\sec^2(z/dR_d)}{c^2 dR_d}$$

$$+\frac{A\omega_{p0}^4 z^2\sec^4(z/dR_d)}{4c^2d^2R_d^2(\omega^2-\omega_{p0}^2\tan(z/dR_d))} \qquad (9.7)$$

To solve equation (9.7) we express A as

$$A(x,y,z)=A_{mn}(x,y,z)\exp[-ikS(x,y,z)] \qquad (9.8)$$

Where, $k=(\omega/c)\varepsilon_0^{1/2}$ and A_{mn} and S depend on x, y and z. Differentiating equation (9.8) w. r. t.' x, y and z, we get

$$\frac{\partial\vec{A}}{\partial x}=Exp[-iKS(x,y,z)]\left[\frac{\partial A_{mn}}{\partial x}-ikA_{mn}\frac{\partial S}{\partial x}\right]$$

$$\frac{\partial^2\vec{A}}{\partial x^2}=Exp[-iKS(x,y,z)]\left[\frac{\partial A^2{}_{mn}}{\partial x^2}-ikA_{mn}\frac{\partial^2 S}{\partial x^2}-2ik\frac{\partial S}{\partial x}\frac{\partial A_{mn}}{\partial x}-k^2A_{mn}\left(\frac{\partial S}{\partial x}\right)^2\right]$$

Similarly,

$$\frac{\partial^2\vec{A}}{\partial y^2}=Exp[-iKS(x,y,z)]\left[\frac{\partial A^2{}_{mn}}{\partial y^2}-ikA_{mn}\frac{\partial^2 S}{\partial y^2}-2ik\frac{\partial S}{\partial y}\frac{\partial A_{mn}}{\partial y}-k^2A_{mn}\left(\frac{\partial S}{\partial y}\right)^2\right]$$

$$\frac{\partial\vec{A}}{\partial z}=Exp[-iKS(x,y,z)]\left[\frac{\partial A_{mn}}{\partial z}-ikA_{mn}\frac{\partial S}{\partial z}-iSA_{mn}\frac{\partial k}{\partial z}\right]$$

Substituting the above values in Eq. (9.7), we get

$$\frac{\partial A^2{}_{mn}}{\partial x^2}+\frac{\partial A^2{}_{mn}}{\partial y^2}-ikA_{mn}\left(\frac{\partial^2 S}{\partial x^2}+\frac{\partial^2 S}{\partial y^2}\right)-2ik\left(\frac{\partial S}{\partial x}\frac{\partial A_{mn}}{\partial x}+\frac{\partial S}{\partial y}\frac{\partial A_{mn}}{\partial y}\right)+\frac{\omega^2\phi(A_{mn}^2)A_{mn}}{c^2}-$$

$$k^2A_{mn}\left[\left(\frac{\partial S}{\partial x}\right)^2+\left(\frac{\partial S}{\partial y}\right)^2\right]=i\left(\frac{2dR_d k^2c^2-\omega_{p0}^2 zSec^2(z/dR_d)}{2kc^2dR_d}\right)\left[\frac{\partial A_{mn}}{\partial z}-ikA_{mn}\frac{\partial S}{\partial z}-iSA_{mn}\frac{\partial k}{\partial z}\right]$$

$$-\frac{iA_{mn}\omega_{p0}^2 Sec^2(z/dR_d)}{kc^2 dR_d}\left[1+\frac{z\omega_{p0}^2}{4k^2c^2dR_d}+\frac{z\tan(z/dR_d)}{dR_d}-ikz+\frac{z\omega_{p0}^2\tan^2(z/dR_d)}{4k^2c^2dR_d}\right]$$

$$+\frac{A_{mn}\omega_{p0}^4 z^2 Sec^4(z/dR_d)}{4k^2c^4d^2R_d^2} \qquad (9.9)$$

Now, equating real and imaginary parts of Eq. (9.9), we get

Real part equation is

$$\frac{1}{\omega^2 A_{mn}}\left(\frac{\partial^2 A_{mn}}{\partial x^2}+\frac{\partial^2 A_{mn}}{\partial y^2}\right)+\frac{\phi(A_{mn}^2)}{\varepsilon_0}=\left(\frac{1}{\omega^2c^2}\right)\left[k^2c^2+\frac{\omega_{p0}^2 zSec^2(z/dR_d)}{2dR_d}\right]\left(\frac{\partial S}{\partial z}\right)+$$

$$\frac{k^2}{\omega^2}\left[\left(\frac{\partial S}{\partial x}\right)^2+\left(\frac{\partial S}{\partial y}\right)^2\right]+\frac{S\omega_{p0}^2 Sec^2(z/dR_d)}{2\omega^2c^2dR_d}\left[\left(1+\frac{z}{S}\right)\left(\frac{\omega_{p0}^2 zSec^2(z/dR_d)}{2dR_dk^2c^2}\right)-1-\frac{2z}{S}\right]$$

(9.10)

Imaginary part equation is

$$A_{mn}^2\left(\frac{\partial^2 S}{\partial x^2}+\frac{\partial^2 S}{\partial y^2}\right)+\frac{\partial S}{\partial x}\frac{\partial A_{mn}^2}{\partial x}+\frac{\partial S}{\partial y}\frac{\partial A_{mn}^2}{\partial y}+\frac{1}{2}\left(1-\frac{\omega_{p0}^2 zSec^2(z/dR_d)}{2dR_dk^2c^2}\right)\left(\frac{\partial A_{mn}^2}{\partial z}\right)-$$

$$\left(\frac{\omega_{p0}^2 A_{mn}^2 Sec^2(z/dR_d)}{dR_dk^2c^2}\right)\left[1+\frac{\omega_{p0}^2 z}{4dR_dk^2c^2}+\frac{\omega_{p0}^2 z\tan^2(z/dR_d)}{4dR_dk^2c^2}+\frac{z\tan(z/dR_d)}{dR_d}\right]=0 \quad (9.11)$$

The solutions of equations (9.10) and (9.11) can be written as:

$$A_{mn}^2=\frac{E_0^2}{f_1(z)f_2(z)}H_m\left(\frac{\sqrt{2}x}{r_0 f_1(z)}\right)H_n\left(\frac{\sqrt{2}y}{r_0 f_2(z)}\right)\exp\left[-\left(\frac{x^2}{r_0^2 f_1^2(Z)}+\frac{y^2}{r_0^2 f_2^2(z)}\right)\right]\times$$

$$\cos\left(\frac{\Omega_0 x}{f_1(z)}\right)\cos\left(\frac{\Omega_0 y}{f_2(z)}\right) \qquad (9.12)$$

And

$$S = \frac{x^2}{2}\beta_1(z) + \frac{y^2}{2}\beta_2(z) + \phi(z) \tag{9.13}$$

Where, $\beta_1(z) = (1/f_1(z))(\partial f_1/\partial z)$ and $\beta_2(z) = (1/f_2(z))(\partial f_2/\partial z)$ represent the curvature of the wavefront in x and y directions respectively. Now, using Eq. (9.12) and Eq. (9.13) in Eq. (9.10) and employing the paraxial approximation, we obtain the expressions for the beam width parameters f_1 and f_2 as follows:

$$\frac{2}{f_1^3}\left(1-\frac{\omega_{p0}^2}{\omega^2}\tan(\xi/d)\right)-\left(\frac{r_0\omega}{c}\right)^2\left(\frac{\omega_{p0}^2}{\omega^2}\right)\left(1-\frac{\omega_{p0}^2}{\omega^2}\tan(\xi/d)\right)\left(\frac{3m}{2M}\right)\left(1+\frac{b^2}{2}\right)\times$$

$$\frac{(\alpha E_0^2)\tan(\xi/d)}{f_1^2 f_2}\exp\left(-\frac{3m\alpha E_0^2}{4Mf_1 f_2}\right)=\left[1-\frac{\omega_{p0}^2}{\omega^2}\tan(\xi/d)+\frac{\omega_{p0}^2\xi\sec^2(\xi/d)}{2d\omega^2}\right]\frac{\partial^2 f_1}{\partial\xi^2}+$$

$$\left[1-\frac{\omega_{p0}^2}{\omega^2}\tan(\xi/d)-\frac{\omega_{p0}^2\xi\sec^2(\xi/d)}{2d\omega^2}\right]\frac{1}{f_1}\left(\frac{\partial f_1}{\partial\xi}\right)^2+\frac{\omega_{p0}^2\sec^2(\xi/d)}{2d\omega^2}\times$$

$$\left[\frac{\omega_{p0}^2\xi\sec^2(\xi/d)}{2d\omega^2\left(1-\frac{\omega_{p0}^2}{\omega^2}\tan(\xi/d)\right)}-1\right]\left(\frac{\partial f_1}{\partial\xi}\right) \tag{9.14}$$

And

$$\frac{2}{f_2^3}\left(1-\frac{\omega_{p0}^2}{\omega^2}\tan(\xi/d)\right)-\left(\frac{r_0\omega}{c}\right)^2\left(\frac{\omega_{p0}^2}{\omega^2}\right)\left(1-\frac{\omega_{p0}^2}{\omega^2}\tan(\xi/d)\right)\left(\frac{3m}{2M}\right)\left(1+\frac{b^2}{2}\right)\times$$

$$\frac{(\alpha E_0^2)\tan(\xi/d)}{f_2^2 f_1}\exp\left(-\frac{3m\alpha E_0^2}{4Mf_1 f_2}\right)=\left[1-\frac{\omega_{p0}^2}{\omega^2}\tan(\xi/d)+\frac{\omega_{p0}^2\xi\sec^2(\xi/d)}{2d\omega^2}\right]\frac{\partial^2 f_2}{\partial\xi^2}+$$

$$\left[1-\frac{\omega_{p0}^2}{\omega^2}\tan(\xi/d)-\frac{\omega_{p0}^2\xi\sec^2(\xi/d)}{2d\omega^2}\right]\frac{1}{f_2}\left(\frac{\partial f_2}{\partial\xi}\right)^2+\frac{\omega_{p0}^2\sec^2(\xi/d)}{2d\omega^2}\times$$

$$\left[\frac{\omega_{p0}^2 \xi \sec^2(\xi/d)}{2d\omega^2\left(1-\frac{\omega_{p0}^2}{\omega^2}\tan(\xi/d)\right)}-1\right]\left(\frac{\partial f_2}{\partial \xi}\right) \tag{9.15}$$

Where, $b = r_0\Omega_0$ is called decentered parameter, $\rho_0 = r_0\omega/c$ is the equilibrium beam radius, $\xi = z/R_d$ is the normalized propagation distance and $R_d = kr_0^2$ represents the diffraction length. Equations (9.14) and (9.15) represent the expressions for the parameters f_1 and f_2 respectively.

9.5 NUMERICAL RESULTS AND DISCUSSION

To compute the above analysis, we solve Eq. (9.14) and Eq. (9.15) by using the initial conditions $[\partial f_1/\partial\xi]_{\xi=0} = 0, [f_1]_{\xi=0} = 1$ and $[\partial f_2/\partial\xi]_{\xi=0} = 0, [f_2]_{\xi=0} = 1$ respectively. The various parameters chosen for the purpose of numerical calculations are as follows:

$\omega = 10^{14} rad/\sec$, $r_0 = 5\times10^{-3} cm$ and $n_0 = 9.98\times10^{17} cm^{-3}$ [71]. The diffractional divergence of the laser beam is due to the diffraction term while as self-focusing is due to nonlinear term. Figures 9.1 (a) and 9.1 (b) represent the dependence of f_1 and f_2 with propagation distance for various values of ω_{p0}/ω with $b = 0$ and 1 respectively. The other parameters are $\alpha E_0^2 = 2$, m/M = 0.02, $r_0\omega/c$ = 50 and d = 10. It is observed from these figures that the beam width parameters attain minimum values at ξ = 4.3 (corresponding to ω_{p0}/ω = 0.8) and ξ = 2.3 (corresponding to ω_{p0}/ω = 0.7) respectively. The amplitude of successive oscillations of f_1 and f_2 decreases and shifts towards lower values of ξ. It means that by considering the ramped density profile and taking in to account the effect of relative plasma density, the self-focusing occurs earlier and becomes stronger. This is due to increase in slope of plasma density curve along the propagation axis. Further, as the laser beam deepens in to the plasma, the plasma dielectric constant decreases rapidly. It is because the electron density depends on the propagation distance. Furthermore, the density ramp causes more reduction in the amplitude of

spot size of laser beam close to the propagation axis. Consequently, the effect gets enhanced and the beam is more focused. However, in uniaxial crystals the HcosG beam spreads in the $x-y$ plane with increasing propagation distance. However, for a short propagation distance its initial beam profile remains invariant [137]. But, in the present communication, it is interesting to note that the oscillatory behavior of f_1 and f_2 is deepened gradually and self-focusing of the laser beam starts acting comparatively at lower values of ξ. Therefore, a desirable self-focusing effect of HcosG beam is observed by exploiting the decentered parameter and hence agrees with the results of Patil *et al.* [73].

Figure 9.2 indicates the variation f_1 and f_2 with ξ for different values of b at ω_{p0}/ω = 0.5. The other parameters are same as taken in figure 9.1(a). It is evident from figure 9.2 that the beam width parameters attain a minimum value at comparatively lower value of ξ = 3.15 corresponding to decentered parameter $b=1.5$. It is due to the fact that as the decentered parameter is increased, the laser spot size of HcosG beam gets reduced under plasma density ramp. Therefore, the beam converges rapidly and focuses to a smaller spot size. This is because of decentered parameter that changes the self-focusing / defocusing nature of beam in a significant manner. Further, it is the important parameter that has to be optimized to get stronger self-focusing and thus supports the results [90]. Figure 9.3 represents the beam width parameters variation with ξ for various values of αE_0^2. The decentered parameter is fixed at $b=1.5$ and the other parameters are same as taken in Figure 9.2. It is obvious from the figure 9.3 that sharp self-focusing is observed at $\xi=3.15$ (corresponding to αE_0^2 = 2). This is because self-focusing term becomes dominant over diffraction term because of the relativistic nonlinearity. It is seen from figure 9.3 that the laser beam becomes self-focused as we increase the initial power of the beam. Hence, in addition to density ramp and decentered parameter, the intensity of laser can be considered to be important in obtaining better focusing of HcosG laser beam.

9.6 CONCLUSION

In the investigation under consideration, we have studied the propagation of Hermite-cosine-Gaussian (HcosG) beam by considering plasma density ramp in a parabolic medium under

paraxial approximation. Our simulation results reveal that the density transition and decentered parameter (b) enhance the self-focusing of HcosG laser beams to a greater extent. It is noticed that the introduction of plasma density ramp makes a remarkable contribution to the process of self-focusing. Moreover, due to increase in the value of intensity of laser beam, self-focusing enhances and shifts towards lower values of normalized distance of propagation. Thus, one may conclude that the optimized laser and plasma parameters have a significant role in improving the focusing of HcosG beam in plasma. The results of present communication could be useful for various applications like plasma-based accelerators and inertial fusion.

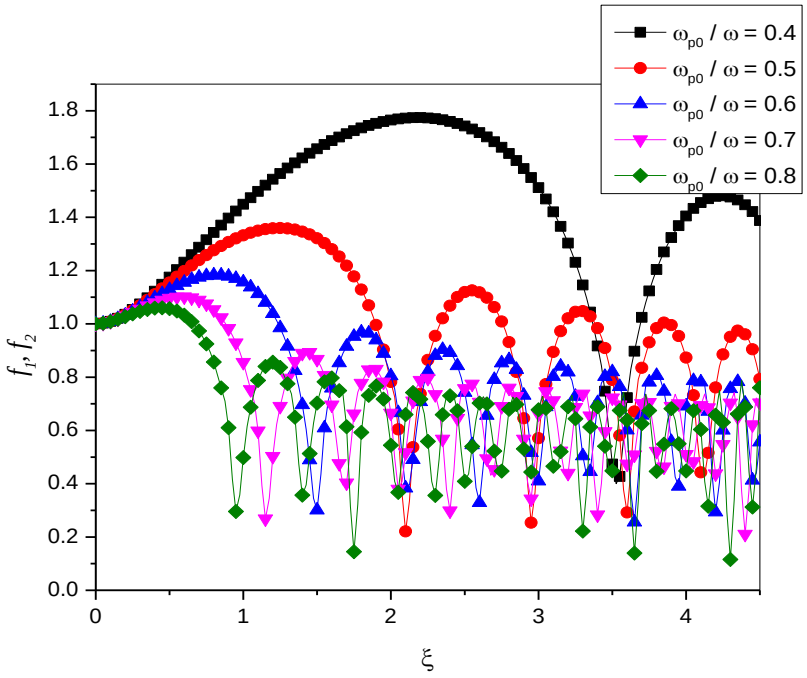

Figure 9.1 (a): Dependence of f_1 and f_2 on ξ for various values of ω_{p0}/ω. The decentered parameter is fixed at $b = 0$ and the other parameters are $\alpha E_0^2 = 2$, $m/M = 0.02$, $r_0\omega/c = 50$ and $d = 10$

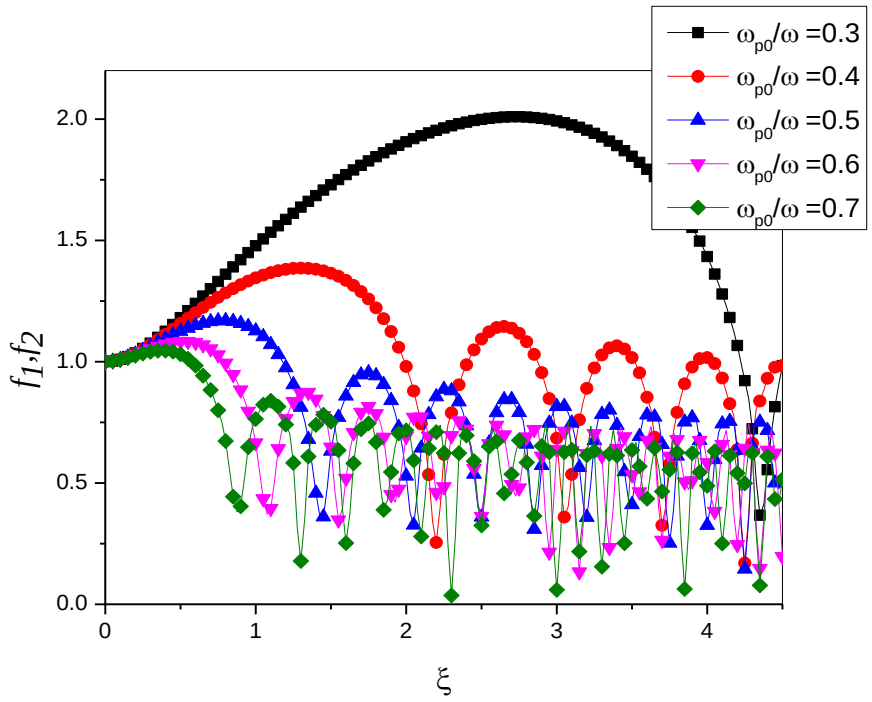

Figure 9.1(b): Dependence of f_1 and f_2 on ξ for various values of ω_{p0}/ω. The decentered parameter is fixed at $b = 1$ and the other parameters are same as taken in Figure 9.1 (a)

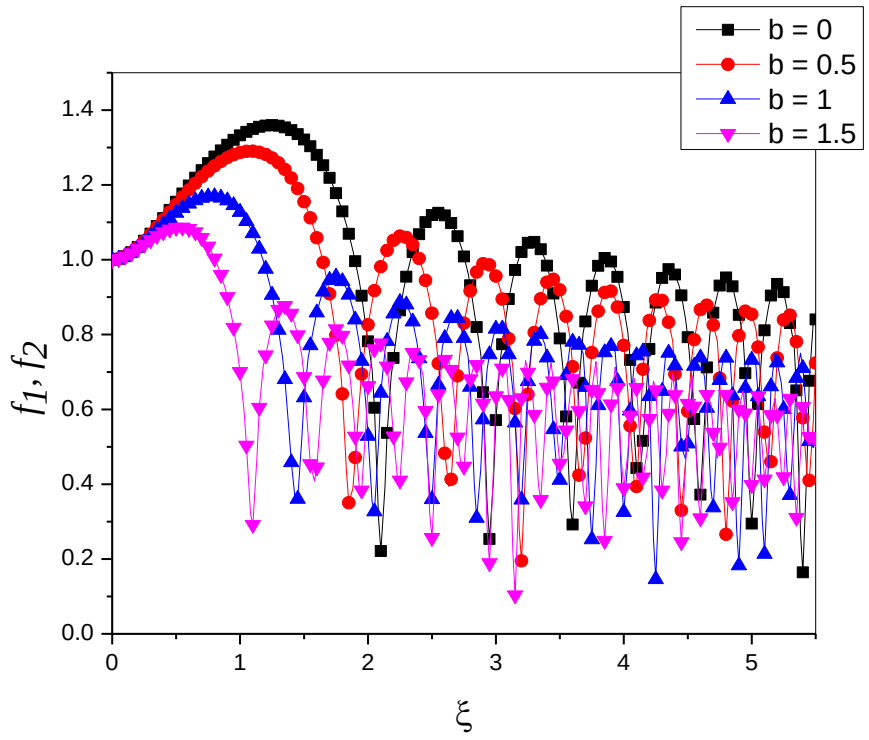

Figure 9.2: Dependence of f_1 and f_2 on ξ for various values of decentered parameter b. The other parameters are: d = 10, $\alpha E_0^2 = 2$, $m/M = 0.02$, $r_0\omega/c = 50$ and $\omega_{p0}/\omega = 0.5$

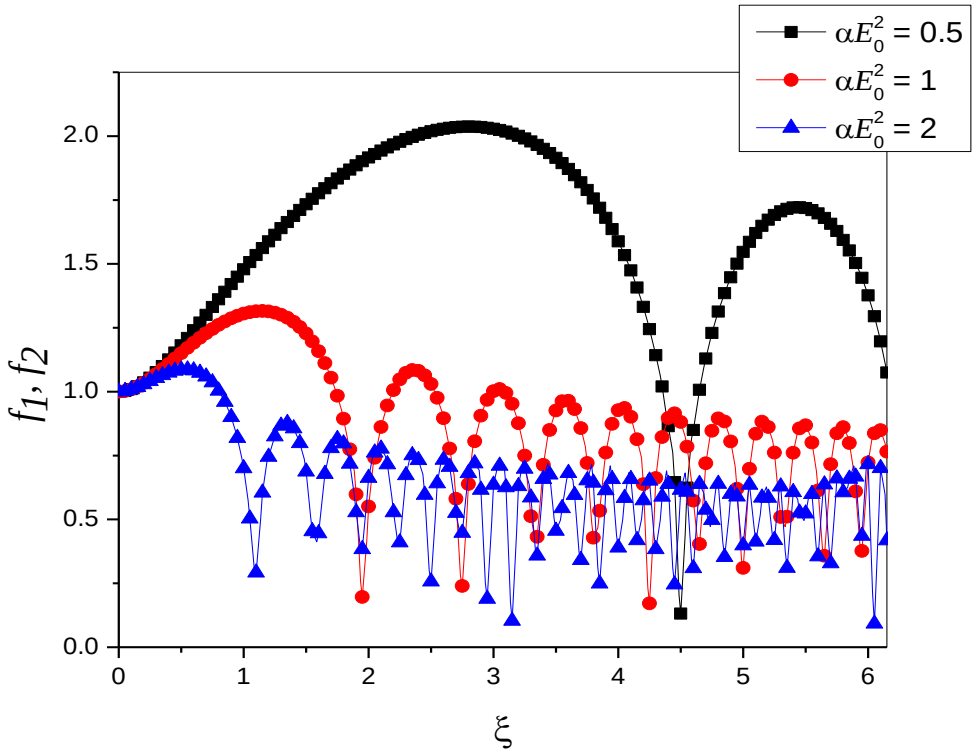

Figure 9.3: Dependence of f_1 and f_2 on ξ for various values of αE_0^2. The decentered parameter is fixed at $b = 1.5$ and the other parameters are same as taken in Figure 9.2